02,08

Experimental investigation of the influence of silver on the properties of bicrystal junction in an HTSC detector

© V.Yu. Safonova^{1,2}, A.E. Parafin², D.V. Masterov², S.A. Pavlov², L.S. Revin^{1,2}

¹ Alekseev State Technical University,

Nizhny Novgorod, Russia

² Institute of Physics of Microstructures, Russian Academy of Sciences,

Nizhny Novgorod, Russia

E-mail: rls@ipmras.ru

Received March 6, 2025

Revised March 6, 2025 Accepted May 5, 2025

The study is focused on investigating the silver film influence on bicrystal junction properties in high-temperature superconductor (HTSC) detectors on the basis of $YBa_2Cu_3O_{7-\delta}$ (YBCO). This work analyzed five chips made in different process cycles. Each chip has three types of Josephson detector structures with log-periodic antennas with different configurations. Main focus is made on comparing critical current, normal resistance and typical voltage at $4\,K$ and $77\,K$. The findings showed that structures with the same Josephson junction dimensions demonstrate considerable difference in parameters. It was found that the deviation of parameters is mainly caused by the proximity of the silver layer to the bicrystal boundary leading to barrier contamination and change of the junction properties.

Keywords: YBaCuO, Josephson junction, log-periodic antenna, silver.

DOI: 10.61011/PSS.2025.06.61705.13HH-25

1. Introduction

High-temperature superconductors (HTSC) based on YBa₂Cu₃O_{7- δ} (YBCO) are of considerable interest for the development of modern detectors [1,2] and mixers [3,4] used for various applications, including radio astronomy, quantum electronics and communication systems. Unlike low-temperature detectors having a record-breaking sensitivity [5,6], the interest in HTSC is primarily associated with an increase in the energy gap in the superconductor excitation spectrum, and with potential improvement of operating parameters in a wider temperature range. This allows external signals with a frequency equal to units of THz to be detected at 50 K [2].

One of the key elements of such devices are Josephson junctions that provide high sensitivity and broadband signal detection. Nonlinear current-voltage curve (CVC) of such junction similar to semiconductor p-n-junction may be used both for variable signal rectification and mixing. In addition, as there is specific Josephson generation, such system will also have other types of interaction with an external variable signal, which is the basis of a wide range of receivers. For communication between the detector sensor and environment, and for effective reception of high-frequency radiation, the Josephson junction is usually integrated in a planar antenna and mounted on a silicon lens. Depending on the detector application, both narrowband [3] and broadband antenna [4] may be used. To improve antenna reception at high frequencies, it is coated with silver, gold and platinum.

However, the HTSC junction parameters may differ considerably in the manufacturing process and materials

to be used [7,8]. Practical application of such structures is complicated by significant variations of structural parameters during manufacturing: properties may vary considerably between chips, which degrades reproducibility of chips.

This study is dedicated to experimental investigation of the influence of silver film on the properties of a bicrystal junction in an HTSC detector. Silver is often used to make ohmic contacts and antennas, but its diffusion into YBCO film may lead to modification of local chemical composition and material structure, which affects negatively the superconducting properties. This is especially important for a weak link region, where even insignificant changes may cause a change of junction properties.

The investigations were performed on five chips made in different process cycles to obtain statistically significant results and make valid conclusions concerning the influence of various factors on the properties of Josephson junctions. Special focus was made on investigating the dependence of the critical current and normal resistance on the type of structure and fabrication aspects.

The aim of the study is to determine the key factors inducing changes of the bicrystal junction properties and to provide recommendations for improving HTSC detector design to increase repeatability of detector parameters.

2. Aspects of structure formation and measurement procedure

Chips with several bicrystal Josephson junction structures were made by magnetron sputtering of YBCO film

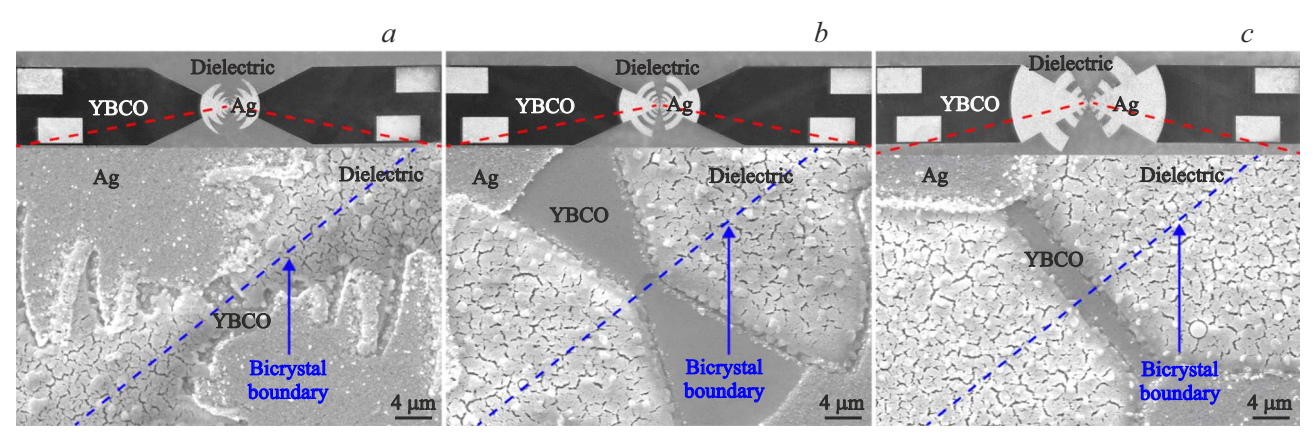


Figure 1. Photographs of three types of Josephson detector structures. Top — full image of the detector with antenna and bonding pads. Bottom — image of Josephson junctions near the interface made by a scanning electron microscope.

onto a $Zr_{1-x}Y_xO_2$ bicrystal substrate with a disorientation angle of 24° in the [001] plane using the master mask method [9]. For broadband communication with external radiation, each junction is integrated with a log-periodic planar antenna [10].

The structures were formed on a cubic zirconia substrate, on which a buffer epitaxial CeO₂ layer was deposited by laser sputtering to ensure lattice matching and reduce chemical interaction between the YBCO and substrate. Layout was created using a master mask: a masking photoresist was made first, then amorphous CeO₂ was deposited by laser sputtering without substrate heating, after which the photoresist and the amorphous CeO2 on it were lifted off leaving openings for YBCO film growth. YBCO film was sputtered at 800–850 °C and Ar(50%)/O₂ mixture pressure of 75 Pa [9]. Detector antenna bonding and ohmic contacts were made by lift-off photolithography using an optical photoresist and thermal silver evaporation. Then the structure was subjected to annealing at 500 °C in oxygen. Josephson junction was formed at the substrate single crystal interface where the superconducting film has low critical current density J_C and critical temperature T_C .

The master mask method was used to avoid degradation of the YBCO film properties minimizing the effect of etching or ion implantation, which is especially important for the weak link region. Thus, high-precision superconducting elements with dimensions equal to some micrometers were created and integrated in log-periodic antennas for broadband signal detection.

Figure 1 shows photographs of three various types of Josephson receivers consisting of log-periodic antennas with various configurations and integrated Josephson junctions. Three structures were fabricated on the same chip (substrate) in a single manufacturing process.

Differences in antenna configurations were caused by the scope of application of the Josephson receivers: frequency band (amplitude frequency response of the antenna, [10]); utilization as a direct detector [11] or mixer [12,13], antenna system size restrictions, etc. Sizes of the Josephson junction (superconducting bridge intersecting the bicrystal

interface) were the same for all types of structures within the accuracy of process resolution ($\sim 3\,\mu\text{m}$). Therefore, transport characteristics of the Josephson junctions were expected to be the same.

A structure in Figure 1, a had a sinusoidal log-periodic antenna with smooth lines of the smallest lobes compared with other antennas. This structure, had a silver (Ag) layer that was placed near the bicrystal boundary shown in Figure 1 as blue dashed lines. The photo shows some local defects of the silver film at the dielectric interface near the dielectric interface.

A structure in Figure 1, b had a larger antenna than that of a structure in Figure 1, a. Layer boundaries on the structure are more distinct, the structure is free of visible damage, dielectric layer and YBCO superconductor maintain their integrity making this structure suitable for practical application.

A structure in Figure 1, c is fitted with a larger antenna with shorter, but wider lobes. By the quality of layers, this structure is similar to that in Figure 1, b, but may slightly differ in the junction width due to the process restrictions.

For convenience of further discussion and an to vividly distinguish these structures, the following designations are assigned to the structures: the structure in Figure 1,a will correspond to type 1, structure in Figure 1,b will correspond to type 2, structure in Figure 1,c will correspond to type 3.

Transport properties of structures were measured in the Gifford–McMahon cryocooler that was used to examine properties in a wide temperature range from 4 to $\sim 80\,K.$ Current-voltage curves were measured by a four-probe method.

3. Analysis of findings

Figure 2 shows the results of investigation of transport properties of three Josephson junction structure types for chip N_2 2 (see Table 1).

At 77 K (Figure 2, a), I_C of structure type 1 is much lower than that of two other structure types and is equal to

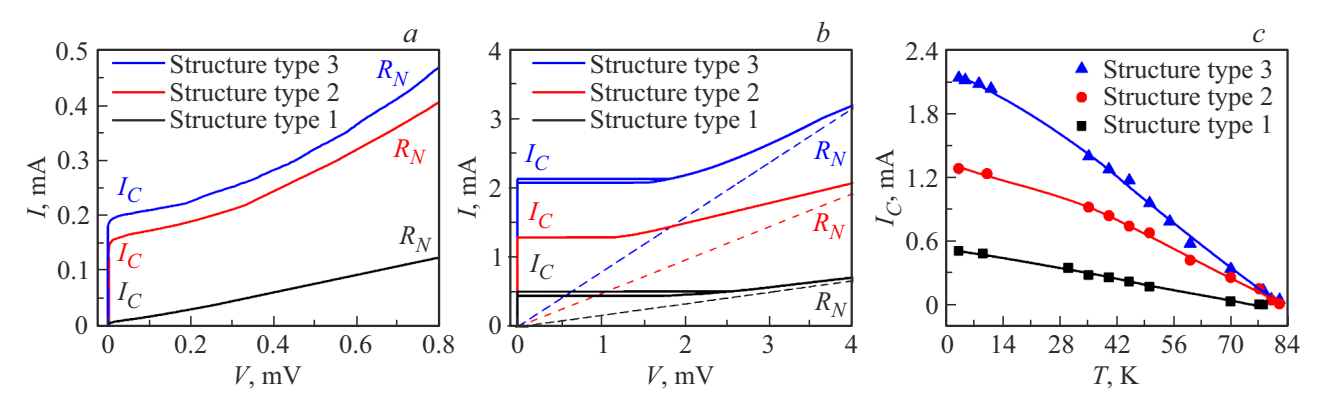


Figure 2. current-voltage curves of three structure types of chip N^{o} 2, measured at 77 K (a) and 4 K (b). c — Dependence of critical current on temperature.

Table 1. Properties of all examined different structure types. L is the Josephson junction length, H is the superconducting film thickness; I_C is the critical current; R_N is the normal resistance; J_C is the critical current density; r_N is the normal resistance normalized to a cross-section area; I_CR_N is the product of the critical current by the normal resistance

Chip	Structure type	L, µm	Η, μm	I_C , mA	R_N , Ohm	J_C , MA/cm ²	r_N , mOhm · cm ²	I_CR_N , mV
№ 1	1	2.85	0.12	0.14	12.1	0.04	2.76	1.70
	2	3.00	0.12	1.15	2.20	0.32	0.53	2.53
Nº 2	1	3.10	0.19	0.52	7.16	0.09	2.81	3.72
	2	3.17	0.19	1.30	1.95	0.22	0.78	2.53
	3	3.07	0.19	2.15	1.32	0.37	0.51	2.84
<u>№</u> 3	2	3.10	0.20	2.05	1.20	0.33	0.50	2.46
№ 4	3	3.10	0.15	2.32	1.20	0.50	0.37	2.78

about $0.02 \,\mathrm{mA}$. Structure type 2 has a critical current close to $0.15 \,\mathrm{mA}$, and the critical current of structure type 3 is much lower than $0.2 \,\mathrm{mA}$. R_N of structure type 2 and 3 at first glance has very close values, while structure type 1 demonstrates a steeper slope of the current-voltage curve, which is indicative of a higher normal resistance.

Figure 2, b shows CVC measured at 4 K. For clarity, resistance of all three types of structures in normal state is shown dashed in the figure. Critical current of structure type 1 was 0.52 mA, of structure type 2 was 1.30 mA, of structure type 3 was 2.15 mA. At a lower temperature, a difference in the critical current between structure types 2 and 3 becomes more clear.

Figure 2, c shows dependences of the critical currents of all structure types on the temperature. The dependence is identical to the experimental observations for other similar structures [14,15]. It can be seen that the critical temperature of structure type 1 is lower that of structure types 2 and 3. In addition, at high temperatures, the critical current measurement error increases due to high fluctuations and pickup, and the difference in values decreases, in particular, this is applicable to structure types 2 and 3. For more detailed measurement analysis, it is reasonable to study CVC at low temperature.

Current-voltage curve measurements were used to calculate the critical current density (J_C) ; normal resistance normalized to the cross-section area (r_N) ; and typical voltage I_CR_N for four chips for more detailed analysis. These properties are normalized to the Josephson junction size, therefore, the structures may be compared with the manufacturing dimensional tolerance. Experimental data for all chips at $4 \, \mathrm{K}$ is listed in Table 1.

According to this data, Figure 3 shows curves of J_C (Figure 3, a), r_N (Figure 3, b) and I_CR_N (Figure 3, c) for three structure types.

Figure 3, a clearly tracks the following dependence: critical current density increases depending on the structure type — from type 1 to type 3. Figure 3, b also demonstrates a dependence, though inverse one: resistivity decreases from structure type 1 to structure type 3. In Figure 3, c, I_CR_N for structure types 2 and 3 demonstrates close values. At the same time, a considerable scatter in values between chips is observed for structure type 1.

Despite the fact that dimensions of three Josephson junction types are close, their properties differ considerably, especially for structure type 1. In addition, structure type 1 features the widest scatter in parameters compared with other structure types. This fact requires more detailed

Chip	Structure type	L, µm	<i>Η</i> , μm	I_C , mA	R_N , Ohm	J_C , MA/cm ²	r_N , mOhm · cm ²	I_CR_N , mV
№ 5	1	3.00	0.08	1.02	2.86	0.42	0.46	2.90
	2	3.80	0.08	1.20	2.51	0.50	0.40	3.00
	3	3.00	0.08	1.38	2.35	0.46	0.48	3.24
0.6						С		
0.0			3.0	_				

Table 2. Properties of three structure types without silver

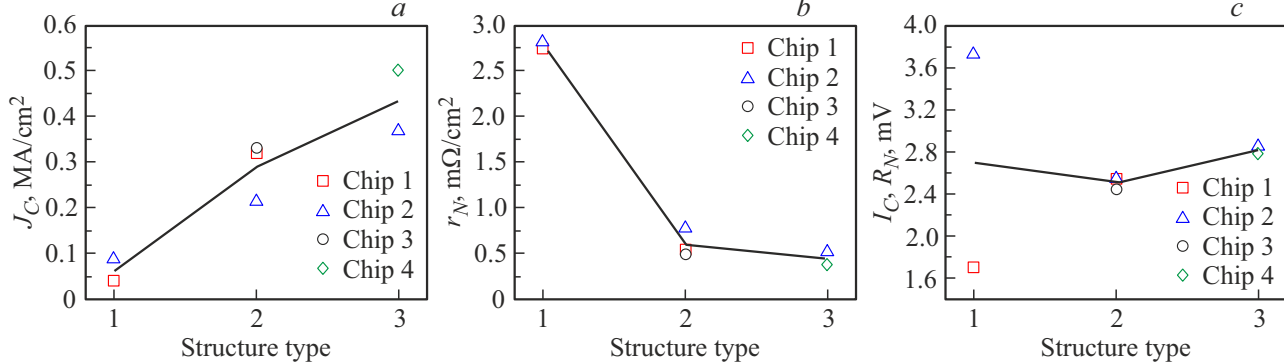


Figure 3. Dependences of critical current density (a), resistivity (b) and typical voltage I_CR_N (c) for three structure types on different chips. Symbols denote the experimental data. Lines are mean values.

review and analysis because understanding of reasons for these differences may be the key factor for improvement of structural properties. In particular, it is necessary to identify whether the observed deviations are caused by the aspects of structure formation, influence of ambient conditions or specific functioning.

4. Influence of silver on the bicrystal junction properties

As a result of analysis and review of possible causes of the observed deviation of parameters, a hypothesis was put forward, according to which this behavior was caused by the influence of silver coating applied to a part of YBCO film near the bicrystal boundary.

Figure. 1, a shows that structure type 1 has a silver (Ag) layer placed in immediate proximity to the bicrystal boundary, unlike two other structure types. Thus, the distance from the bicrystal junction to the silver layer for structure type 1 is approx. $4\mu m$, and for structure types 2 and 3 is $20-30\mu m$. Moreover, partial failure and inhomogeneous silver layer distribution is observed for structure type 1, which may be caused by manufacturing defects or external impacts.

Silver has high diffusion capability and silver atoms in certain conditions may actively penetrate adjacent layers, in particular, the YBCO film [16]. This may lead to formation of nonsuperconducting phases, thick grain boundaries, and formation of structures preventing vortex motion. Silver diffusion may also cause degradation of weak link at the single crystal interface reducing its homogeneity and increasing the concentration of defects.

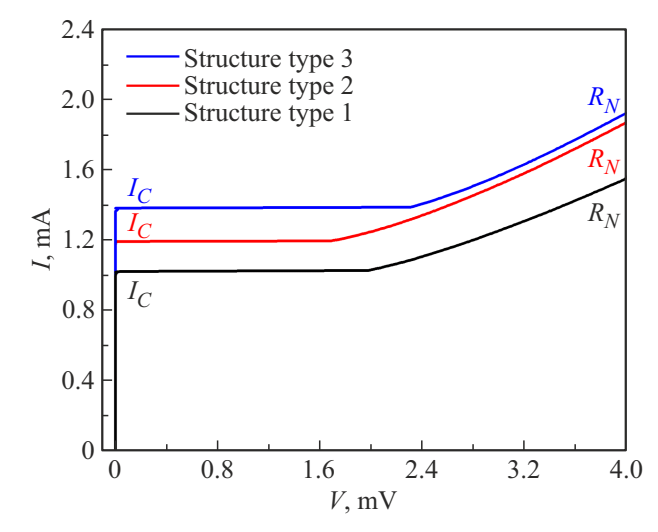


Figure 4. Current-voltage curves of three structure types on chip without silver at 4 K.

This assumption was used as the basis for fabricating the fifth chip with structures identical to the previous ones, but without silver coated antennas. Figure 4 shows CVC of structures without a silver layer measured at 4 K. Analysis of Table 2 shows that transport properties for all three structure types are similar and the scatter in current density and normalized resistance is 10% on average. Therefore, a conclusion may be made that exclusion of silver facilitated normalization of the critical current and normal resistance as well as of typical voltage of the Josephson junction.

5. Conclusion

The investigations have shown that an HTSC detector configuration, including a log-periodic antenna geometry, may have significant influence on the bicrystal junction properties. It was found that samples with the same Josephson junction dimensions could demonstrate considerable differences in the critical current and normal resistance, which is attributable to structural design and aspects of structure formation. The silver film deposited to the antenna and located near the bicrystal boundary exerts the main influence on the junction parameters Silver may cause barrier contamination and modification of junction properties, which is confirmed by the experimental data.

Exclusion of silver from manufacturing of new structures made it possible to improve the repeatability of properties. Critical current and normal resistance for various structure types exhibited close values during measurements, which confirmed the proposed hypothesis concerning the influence of silver.

Thus, the investigations suggest that detector configuration control and exclusion of silver influence are the key factors for improvement the stability of bicrystal junction properties. On the other hand, utilization of silver may be useful to some extent because it allows the junction properties to be modified without considerable degradation (I_CR_N) at low temperatures. Thus, an increase in normal resistance for structure type 1 provides better matching with electro-dynamic environment and better reception properties in the broadband detection mode as reported in [11].

Funding

The study was supported by grant No. 20-79-10384-P.

Conflict of interest

The authors declare that they have no conflict of interest.

References

- O. Volkov, V. Pavlovskiy, I. Gundareva, R. Khabibullin, Y. Divin. IEEE Trans. Terahertz Sci. Technol. 11, 330 (2021).
- [2] V.V. Pavlovskiy, I.I. Gundareva, O.Y. Volkov, Y.Y. Divin. Appl. Phys. Lett. 116, 082601 (2020).
- [3] J. Du, A.R. Weily, X. Gao, T. Zhang, C.P. Foley, Y.J. Guo. Supercond. Sci. Technol. **30**, 024002 (2017).
- [4] D. Cunnane, J.H. Kawamura, N. Acharya, M.A. Wolak, X.X. Xi, B.S. Karasik. Appl. Phys. Rev. 109, 112602 (2016).
- [5] I.I. Soloviev, N.V. Klenov, S.V. Bakurskiy, A.L. Pankratov, L.S. Kuzmin. Appl. Phys. Lett. 105, 202602 (2014).
- [6] V.P. Koshelets, P.N. Dmitriev, A.B. Ermakov, A.S. Sobolev, A.M. Baryshev, P.R. Wesselius, J. Mygind. Supercond. Sci. Technol. 14, 1040 (2001).
- [7] I.I. Gundareva, O.Y. Volkov, M.V. Lyatti, Y.Y. Divin, V.N. Gubankov, V.V. Pavlovskiy. IEEE Trans. Appl. Supercond. 21, 147–150 (2011).

- [8] M.A. Tarasov, E.A. Stepantsov, M. Naito, A. Tsukada, D. Winkler, A.S. Kalabukhov, M.Yu. Kupriyanov. J. Exp. Theor. Phys. 105, 636641 (2007).
- [9] D.V. Masterov, A.E Parafin, L.S. Revin, A.V. Chiginev, E.V. Skorokhodov, P.A. Yunin, A.L. Pankratov. SUST 30, 2, 025007 (2017).
- [10] E.I. Glushkov, A.V. Chiginev, L.S. Kuzmin, L.S. Revin. Beilstein J. Nanotechnol. 13, 325–333 (2022).
- [11] E.A. Matrozova, D.V. Masterov, S.A. Pavlov, A.E. Parafin, L.S. Revin. Zhurnal radioelektroniki 12, 1–11 (2022). (in Russian).
- [12] M.A. Galin, L.S. Revin, A.V. Samartsev, M.Yu. Levichev, A.I. Elkina, D.V. Masterov, A.E. Parafin. ZhTF, 94 (7), 2024 (2024). (in Russian).
- [13] V.A. Anfertiev, D.V. Masterov, A.E. Parafin, L.S. Revin. FTT **66**, 6 (2024). (in Russian).
- [14] E. Il'ichev, V. Zakosarenko, R.P.J. IJsselsteijn, H.E. Hoenig, H.-G. Meyer, M.V. Fistul, P. Müller. Phys. Rev. B 59, 11502-11505 (1999).
- [15] J. Du, A.R. Weily, X. Gao, T. Zhang, C.P. Foley, Y.J. Guo. SUST 30, 024002 (2017).
- [16] J. Joo, J.P. Singh, R.B. Poeppel, A.K. Gangopadhyay, T.O. Mason. J. Appl. Phys. 71, 2351 (1992).

Translated by E.Ilinskaya